Excited-State Intermolecular Proton Transfer Reactions of 7-Azaindole(MeOH) n (n = 1−3) Clusters in the Gas phase: On-the-Fly Dynamics Simulation

ARTICLE *in* THE JOURNAL OF PHYSICAL CHEMISTRY A · DECEMBER 2011

Impact Factor: 2.69 · DOI: 10.1021/jp2059936

6 AUTHORS, INCLUDING:

Nawee Kungwan
Chiang Mai University
55 PUBLICATIONS **217** CITATIONS
SEE PROFILE

Peter Wolschann
University of Vienna
228 PUBLICATIONS **2,149** CITATIONS
SEE PROFILE

Adélia J A Aquino
University of Vienna
93 PUBLICATIONS **1,993** CITATIONS
SEE PROFILE

Mario Barbatti
Aix-Marseille Université
129 PUBLICATIONS **2,698** CITATIONS
SEE PROFILE

THE JOURNAL OF PHYSICAL CHEMISTRY A

ARTICLE

pubs.acs.org/JPCA

Excited-State Intermolecular Proton Transfer Reactions of 7-Azaindole(MeOH)$_n$ (n = 1−3) Clusters in the Gas phase: On-the-Fly Dynamics Simulation

Rathawat Daengngern,[†] Nawee Kungwan,*[,†,‡] Peter Wolschann,[§] Adélia J. A. Aquino,[§] Hans Lischka,[§,∥] and Mario Barbatti[⊥]

[†]Department of Chemistry, Faculty of Science, Chiang Mai University, Chiang Mai 50200, Thailand

[‡]Materials Science Research Center, Faculty of Science, Chiang Mai University, Chiang Mai 50200, Thailand

[§]Institute for Theoretical Chemistry, University of Vienna, Währingerstrasse 17, A-1090 Vienna, Austria

[∥]Department of Chemistry and Biochemistry, Texas Tech University, Lubbock, Texas 79409-1061, United States

[⊥]Max-Planck-Institut für Kohlenforschung, Kaiser-Wilhelm-Platz 1, D-45470, Mülheim an der Ruhr, Germany

Supporting Information

ABSTRACT: Ultrafast excited-state intermolecular proton transfer (PT) reactions in 7-azaindole(methanol)$_n$ (n = 1−3) [7AI(MeOH)$_{n=1-3}$] complexes were performed using dynamics simulations. These complexes were first optimized at the RI-ADC(2)/SVP-SV(P) level in the gas phase. The ground-state structures with the lowest energy were also investigated and presented. On-the-fly dynamics simulations for the first-excited state were employed to investigate reaction mechanisms and time evolution of PT processes. The PT characteristics of the reactions were confirmed by the nonexistence of crossings between $S_{\pi\pi^*}$ and $S_{\pi\sigma^*}$ states. Excited-state dynamics results for all complexes exhibit excited-state multiple-proton transfer (ESmultiPT) reactions via methanol molecules along an intermolecular hydrogen-bonded network. In particular, the two methanol molecules of a 7AI(MeOH)$_2$ cluster assist the excited-state triple-proton transfer (ESTPT) reaction effectively with highest probability of PT.

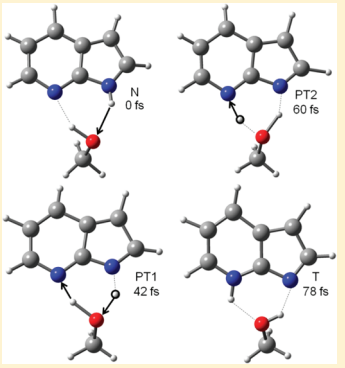

1. INTRODUCTION

Understanding the excited-state proton/hydrogen-atom transfer (ESPT/HT) reaction is a fundamental piece of knowledge in chemistry and biochemistry.[1,2] The ESPT/HT reaction has been intensively studied due to its practical uses in many applications, particularly fluorescent probes,[3−7] dyes,[8,9] photostabilizers,[10] and also light-emitting devices.[11,12] Most of the PT and HT reactions take place in molecules having bifunctional groups[13−17] (proton donor and acceptor) in which these molecules can form intramolecular hydrogen bonds between two functional groups. However, the excited-state intramolecular PT/HT reaction cannot spontaneously occur in some molecules because the proton donor is positioned too far from the acceptor.[15] In such situations, solvent molecules may trigger the ESPT/HT reactions. In the presence of solvent assistance, the formation of strong hydrogen bonds along the hydrogen-bonded network can reduce the reaction barrier and induce intermolecular multiple-PT/HT reactions to take place after the photoexcitation. Simple model compounds of certain molecules with appropriate protic solvents show this kind of process, for instance, 1*H*-pyrrolo[3,2-*h*]quinoline (PQ),[15,17−20] 7-hydroxyquinoline (7HQ),[21−23] and 7-azaindole (7AI).[13,16,17,24−31]

Most previous reports[13,15−17,31] have paid much attention to the 7AI molecule because of its simple structure. It has been employed as a model compound to reveal a key reaction for chemical mutagenesis of DNA base pairs,[32] and it is an important bicyclic azaaromatic molecule consisting of pyrrole (proton donor) and pyridine (proton acceptor) rings. The 7AI with solvent clusters, which have been extensively studied in solvents such as ammonia,[33] water,[13,27,28,31,34−37] and alcohol (especially ethanol[38] and methanol[24,29,30,39−41]), are prototypes for understanding the ESPT/HT reactions. In addition, theoretical calculations of model compounds consisting of 7AI and solvents can be employed to clarify mechanistic aspects of the reaction.

Recently, Sakota et al.[29,30,37,39,40] studied 7AI and its clusters both experimentally and theoretically to obtain information on the PT/HT reaction using a supersonic jet-cool apparatus and structure calculations. Their results, as evidenced by IR-UV ion-dip spectroscopy, showed that the ESPT/HT reactions occurred by solvent-induced molecules involving a cooperative hydrogen-bonded network in 7AI(MeOH)$_{n=1-3}$ clusters. In addition, they found that the observation of the visible fluorescence due to the multiple-PT/HT transfer is cluster-size selective; the 7AI-(MeOH)$_2$ complex undergoes excited-state triple PT/HT

Received: June 25, 2011
Revised: October 22, 2011
Published: October 25, 2011

(ESTPT/HT) reaction efficiently along the hydrogen-bonded network.[30] Their data on the ESPT/HT reaction, however, could not provide information on dynamical aspects, particularly reaction pathways and time evolution[42−46] in the ultrafast time scale. Dynamics simulations can be employed to explore this challenging system to understand the ESPT/HT mechanism, as have been done, for example, by Kina et al.,[31] who used ab initio molecular dynamics simulation (AIMD) for studying the ESPT reaction of $7AI(H_2O)_n$ clusters in the gas phase and in water solution. Their results showed that the H (proton) transferred from H_2O to 7AI via the N···H hydrogen bond around 50 fs in the $7AI(H_2O)_1$ cluster, and the triple-H-transfer occurs in the time range of 40−60 fs in the $7AI(H_2O)_2$ cluster. The detailed information obtained from their work is an excellent example of how theoretical investigations can provide more elaborated dynamic pictures at the molecular level than experimental results alone can in the case of ESPT reaction of $7AI(H_2O)_n$ clusters. Therefore, the combination of both methods[31,37] can serve as a powerful tool to clarify detailed mechanisms of PT/HT processes. The processes in the excited state can exhibit either PT or HT features depending upon the energy order of the $S_{\pi\pi^*}$ and $S_{\pi\sigma^*}$ in the target systems. These states play important roles in determining the nature of the excited-state reactions: protons are transferred along the $S_{\pi\pi^*}$ state, whereas hydrogen atoms are transferred along the $S_{\pi\sigma^*}$ state.[22,47−49] Particularly, it has been pointed out in previous investigations on the energy paths[37,50] that the $S_{\pi\sigma^*}$ state lies well above the $S_{\pi\pi^*}$ state with no intersections.

In this work, we have investigated the ESPT reactions occurring through methanol-assisted molecules on the hydrogen bond network of $7AI(MeOH)_n$ (where n = 1−3) complexes. To the best of our knowledge, the PT/HT dynamics of these complexes has not been theoretically studied before. A similar system, the $7AI(H_2O)_n$ cluster, has been well studied by Kina et al.[31] By substituting water with methanol into 7AI, we expect there to be a similarity in PT/HT dynamics information since methanol is a polar solvent like water. However, water is more polar than methanol, so one could anticipate that the time evolution of PT/HT in $7AI(MeOH)_n$ is slower than that in $7AI(H_2O)_n$. To gain insight into structural aspects, the ground-state structures were acquired prior to dynamics simulation. On-the-fly dynamics simulation[42,43,45,51,52] was employed to obtain mechanistic information on the $7AI(MeOH)_{n=1-3}$ clusters reactions. We present both static and dynamics calculations for different methanol cluster sizes. The reaction pathways in which the transfer occurs, the $S_{\pi\pi^*}$ state for the $7AI(MeOH)_{n=1-3}$ clusters, are also analyzed in detail.

2. COMPUTATIONAL DETAILS

2.1. Ground-State Calculations. The structures of $7AI(MeOH)_{n=1-3}$ complexes ground state were first optimized in the gas phase with the quantum chemical program package TURBOMOLE 5.10.[53,54] The resolution-of-the-identity approximation[55] for the electron repulsion integrals and algebraic diagrammatic construction[56] through the second-order method RI-ADC(2) was used for geometry optimizations. For polyatomic molecules, the ADC(2) calculations gave almost the same accuracy as obtained by the coupled-cluster singles-and-doubles (CC2) model[49] and were also less time consuming than those computed with CC2.[42] The split valence polarized (SVP) basis set[57] was assigned to heavy atoms and to hydrogen atoms involved in the hydrogen-bonded network, whereas the split valence (SV(P)) basis set was assigned to the remaining hydrogen atoms in the complexes. This mixed basis set, which will be referred to throughout this paper as SVP-SV(P), is designed to keep the computational costs for the dynamics at an acceptable level but still provides accurate results for the 7AI and methanol systems. The minimum character of all optimized structures of $7AI(MeOH)_{n=1-3}$ were confirmed by normal-mode analysis at the same basis set level, also further used for excited-state dynamics simulations.

2.2. Excited-State Dynamics Simulations. Classical dynamics simulations were carried out for the $7AI(MeOH)_{n=1-3}$ complexes on the first-excited state (S_1) energy surface using the ADC(2) method with SVP-SV(P) as is used in the ground-state calculations. The ground-state geometries of each complex were prepared prior to initial condition generation. The initial conditions were generated using a harmonic-oscillator Wigner distribution for each normal mode,[58] as implemented in the NEWTON-X program package[51,59] interfaced with the TURBOMOLE program. A hundred trajectories for each complex were simulated with a time step of 1 fs and the maximum time up to 300 fs. For a selected trajectory of each complex, characteristic points along the reaction pathways, namely, normal (N), intermediary structure (IS), and tautomer (T) were selected for further analysis. The N point was chosen at the time of 0 fs. The IS point was identified at the time of proton being translocated to complete the PT process. The T point was selected right after the PT process (tautomerization) was completed. Molecular orbital characterization of the different electronic transitions was performed to verify the PT or HT pathways involved in the reactions. Furthermore, a statistical analysis was also carried out to give detailed properties (e.g., energies and internal coordinates), which were used to obtain time evolution of the PT/HT reactions along the hydrogen-bonded network.

3. RESULTS AND DISCUSSION

3.1. Ground-State Structures. The optimized structures of 7AI with methanol clusters are depicted in Figure 1 with numbering atoms of intermolecular hydrogen-bonded networks. To understand the surrounding cooperative methanol molecules on the intermolecular hydrogen bonds of the complexes, the ground-state structures of $7AI(MeOH)_{n=1-3}$ complexes were optimized using the RI-ADC(2)/SVP-SV(P) level. Intermolecular hydrogen bonds between 7AI and methanol molecules presented as dashed lines, selected distances, and dihedral angles are summarized in Table 1.

One methanol molecule is added into the 7AI molecule forming a $7AI(MeOH)_1$ complex as shown in Figure 1a. It is found that the 7AI acts as a proton donor (pyrrole ring) and a proton acceptor (pyridine ring). Typically, there are two intermolecular hydrogen bonds labeled as R_1(H1···O1) with a bond distance of 1.967 Å and R_2(H2···N2) with a bond distance of 1.921 Å. The SVP basis set assigned to atoms involved in the hydrogen-bonded network is able to describe the nature of the hydrogen bond well, resulting in intermolecular hydrogen bond formation between 7AI and methanol. When two methanol molecules are added into 7AI, a new complex is formed (illustrated in Figure 1b). The optimized structure of a $7AI(MeOH)_2$ complex shows that there are three intermolecular hydrogen bonds in the cyclic network: first, the hydrogen bond formation between a proton donor on a pyrrole ring of 7AI and

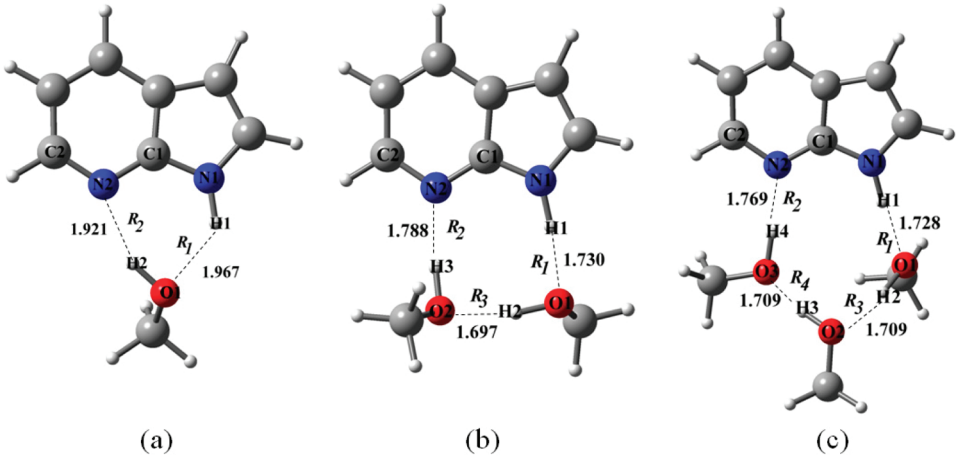

Figure 1. The ground-state optimized structures of 7AI(MeOH)$_n$ (where $n = 1-3$) complexes at the RI-ADC(2)/SVP-SV(P) level. Numbering atoms for intermolecular hydrogen bonds to methanol molecules (a) 7AI(MeOH)$_1$ (b) 7AI(MeOH)$_2$ and (c) 7AI(MeOH)$_3$. Intermolecular hydrogen-bonded interactions are shown as dashed lines (Å).

Table 1. Summary of Intermolecular Hydrogen Bonds and Selected Distances (Å) and øN1C1N2C2 Dihedral Angles (°) of the Ground-State Structures Performed at the RI-ADC(2)/SVP-SV(P) Level (MP2 Level in Parentheses[39])

	complex		
	7AI (MeOH)$_1$	7AI (MeOH)$_2$	7AI (MeOH)$_3$
R_1	1.967	1.730	1.728
	(2.02)	(1.81)	(1.78)
R_2	1.921	1.788	1.769
	(1.94)	(1.80)	(1.76)
R_3		1.697	1.709
		(1.74)	(1.72)
R_4			1.709
			(1.70)
N1−O1	2.799	2.765	2.768
O[a]−N2	2.820	2.767	2.768
O1−O2		2.661	2.675
O2−O3			2.674
ø	179.9	179.8	180.0

[a] O1 for one methanol, O2 for two methanol, and O3 for three methanol.

the first methanol (1.730 Å), second, the second methanol to a proton acceptor on a pyridine ring of 7AI (1.788 Å), and third, between two methanol molecules (1.697 Å) for R_1(H1···O1), R_2(H3···N2), and R_3(H2···O2), respectively. By increasing the number of methanol molecules, the intermolecular hydrogen bonds become stronger (the hydrogen bonds are shorter) due to dispersion interaction between 7AI and methanol. Both R_1 and R_2 of the 7AI(MeOH)$_2$ cluster are shorter than those of the 7AI(MeOH)$_1$ cluster by 0.237 and 0.133 Å, respectively, indicating that the number of methanol molecules plays a role in the structural stability. Moreover, the optimized structure of a 7AI(MeOH)$_3$ cluster as shown in Figure 1c has four intermolecular hydrogen bonds R_1(H1···O1), R_2(H4···N2), R_3(H2···O2), and R_4(H3···O3), whose bond distances are 1.728, 1.769, 1.709, and 1.709 Å, respectively. For the hydrogen bonds between two methanol molecules (R_3 and R_4), the bond distances are the same. The R_3 bond is longer than that of the 7AI(MeOH)$_2$ cluster by only 0.01 Å. Increasing the number of methanol molecules increases the intermolecular hydrogen bond strength between 7AI and methanol, as can be noted by the systematic shrink of R_1 and R_2 with the increase of the cluster size.

The study of the IR-dip spectra[39] showed that the cooperative effect of hydrogen bond formation in further sites may be saturated in 7AI(MeOH)$_n$ ($n > 3$). In addition, the optimizations of three clusters at the RI-ADC(2)/SVP-SV(P) level show that the intermolecular hydrogen bonds are slightly shorter than previously reported by Sakota et al. computed at the MP2 level (Table 1). For example, R_1 and R_2 bonds of a 7AI(MeOH)$_1$ cluster show shorter intermolecular distances by 0.05 and 0.02 Å, respectively, as well as a 7AI(MeOH)$_2$ complex with R_1(0.08 Å), R_2(0.01 Å), and R_3(0.04 Å) bonds. Hydrogen bonds R_1 and R_3 of 7AI(MeOH)$_3$ show shorter distances by 0.05 and 0.01 Å, whereas R_2 and R_4 bonds show slightly longer distances by 0.01 Å. The 7AI structure for each cluster is totally planar, confirmed by a dihedral angle (øN1C1N2C2) of 180°. The structural information of 7AI(MeOH)$_{n=1-3}$ clusters calculated at the RI-ADC(2)/SVP-SV(P) level in this present study agrees well with high accurate MP2/6-31++G**/6-31G* calculations with the basis set superposition error (BSSE) by Sakota et al.[39] Thus, the optimized structures of the 7AI(MeOH)$_{n=1-3}$ complexes at the RI-ADC(2)/SVP-SV(P) level will be used in excited-state dynamics simulations to obtain detailed information on the PT/HT dynamics properties. The types of excited-state PT/HT on 7AI(MeOH)$_n$ are double, triple, and quadruple PT/HT reaction when $n = 1$, 2, and 3, respectively.

3.2. Excited-State Dynamics Simulations. One hundred trajectories of on-the-fly dynamics simulations are generated for each complex to investigate the PT/HT pathway. The analysis using simulation times up to 300 fs should reveal the mechanism including pre- and post-PT/HT processes. By definition, the PT/HT time from atom X to atom Y is taken as the time for which the X−H distance becomes equal to the H−Y distance.[43,45,50] The trajectories for each complex of 7AI(MeOH)$_{n=1-3}$ were classified and divided into three types of reactions: (1) ESPT with a proton being transferred within a given simulation time of 300 fs, (2) stopped

Table 2. Summary of the Excited-State Dynamics Analysis of 7AI(MeOH)$_{n=1-3}$ Complexes[a]

	reaction (in trajectory)				time (fs)			
complex	ESPT ($S_{\pi\pi^*}$)	stopped ($S_{\pi\pi^*}/S_{\pi\sigma^*}$)	no	probability[b]	PT1	PT2	PT3	PT4
7AI(MeOH)$_1$	54	13	33	54	71	84		
					(1.361)	(1.379)		
7AI(MeOH)$_2$	67	6	27	67	57	70	83	
					(1.297)	(1.295)	(1.341)	
7AI(MeOH)$_3$	26	14	60	26	66	77	83	84
					(1.301)	(1.229)	(1.270)	(1.338)

[a] Average distance (Å) of X−H and H−Y intersection for each PT (in parentheses). [b] Reaction probability (%).

Table 3. Relative Ground (S_0) and Excited State ($S_{\pi\pi^*}$, $S_{\pi\sigma^*}$) Energies (kcal·mol^{-1}) for Characteristic Stationary Points of Normal (N), Intermediary Structure (IS), and Tautomer (T) along the Reaction Pathways of One Selected Trajectory of Each Complex[a]

		complex		
state	form	7AI (MeOH)$_1$	7AI (MeOH)$_2$	7AI (MeOH)$_3$
S_0	N	0.00	0.00	0.00
	IS	57.02	47.20	49.58
	T	15.81	10.85	13.83
$S_{\pi\pi^*}$	N	94.09	119.32	99.86
	IS	139.03	123.57	142.08
	T	94.96	98.30	88.99
$S_{\pi\sigma^*}$	N	194.23	189.54	149.99
	IS	237.66	227.29	193.00
	T	201.90	206.30	184.63

[a] Performed at RI-ADC(2)/SVP-SV(P) level.

with $S_{\pi\pi^*}/S_{\pi\sigma^*}$ crossing, and (3) no proton being transferred within a given simulation time of 300 fs. The number of trajectories for each type of reaction, the probability of PT, and the average time of PT for each complex 7AI(MeOH)$_{n=1-3}$ are summarized in Table 2.

We have compared the energies (kcal·mol^{-1}) of the ground (S_0) and the first-excited states ($S_{\pi\pi^*}$ and $S_{\pi\sigma^*}$) for characteristics points along the reaction pathways (Table 3), namely, normal (N), intermediary structure (IS), and tautomer (T) of selected trajectories for each complex. The potential energy diagram of a selected trajectory for a 7AI(MeOH)$_2$ cluster is shown in Figure 2, and the potential energy diagram of selected trajectories for 7AI(MeOH)$_1$ and 7AI(MeOH)$_3$ are shown in Figures S1 and S2 in the Supporting Information. The results of 7AI(MeOH)$_2$ in Table 3 and Figure 2 show that that $S_{\pi\sigma^*}$ lies above the $S_{\pi\pi^*}$ state over 100 kcal·mol^{-1}. No crossing between $S_{\pi\pi^*}$ and $S_{\pi\sigma^*}$ states was observed, and all trajectories evolved along the $S_{\pi\pi^*}$ state, which characterizes the transfer as a PT process. Therefore, the processes in 7AI(MeOH)$_{n=1-3}$ complexes are most likely the ESPT pathway.

To relate the probability of PT with the barrier height of PT in each 7AI(MeOH)$_{n=1-3}$ complex, the relative energies of S_0 and $S_{\pi\pi^*}$ are considered. In the ground state, relative energies of normal forms are lower than those of tautomers, reflecting that normal forms are more stable than the tautomers, and the PT processes are not likely to proceed easily because of high barriers

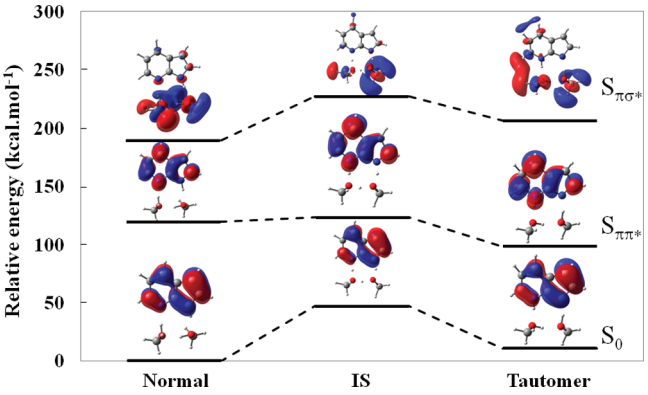

Figure 2. Potential energy diagram of a selected trajectory for a 7AI-(MeOH)$_2$ complex at ground state (S_0) and excited states ($S_{\pi\pi^*}$, $S_{\pi\sigma^*}$) performed at the RI-ADC(2)/SVP-SV(P) level.

around 50 kcal·mol^{-1} for 7AI(MeOH)$_n$. In contrast, the relative energies of normal forms after photoexcitation are higher than those of the tautomers, and they can proceed to the tautomers more easily because of lower barrier height. For the selected trajectories, excited-state barrier heights are found to be 44.94, 4.25, and 42.22 kcal·mol^{-1} for 7AI(MeOH)$_n$ when n = 1, 2, and 3, respectively. Because the barrier heights are calculated from only one selected trajectory for each complex, their values cannot reveal the probability of PT in 7AI(MeOH)$_{n=1-3}$ complexes. However, inferences about the barriers could be made by considering the probabilities of PT in complexes that are averaged based on all ESPT trajectories. From Table 2, given that n = 2 has the highest probability of PT (67%), this implies that the barrier for n = 2 should be the lowest one. This lowest barrier with the highest probability might be due to its shortest distance between N1 and O1 atoms (Figure 1), 1.297 Å (Table 2), in which the PT is more readily translocated from the proton donor to the acceptor. However, the addition of three methanol molecules to 7AI affects the arrangement of a hydrogen-bonded network. This effect could possibly deactivate PT by raising the reaction barrier height, which results in low probability of only 26%.

3.2.1. 7AI(MeOH)$_1$ Complex. From 100 trajectories of a 7AI-(MeOH)$_1$ cluster, 54 out of 87 trajectories showed excited-state double proton transfer (ESDPT) reaction but the PT process did not take place during the simulation time in 33 trajectories. Thirteen trajectories achieved a region of degeneracy between $S_{\pi\pi^*}$ and $S_{\pi\sigma^*}$ and could not be continued because of limitation of the current method. These trajectories can, in principle, be the

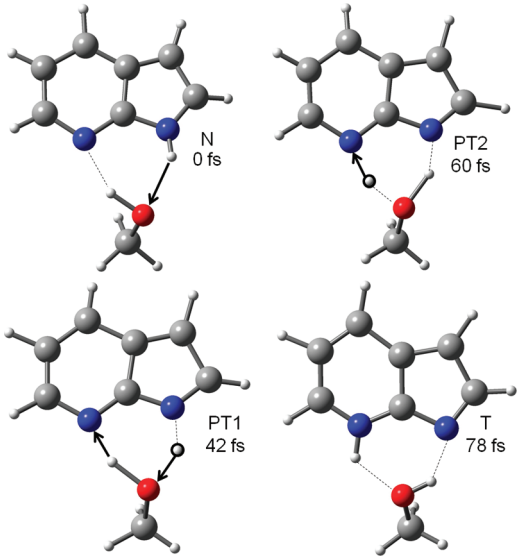

Figure 3. Snapshots for a selected trajectory of a 7AI(MeOH)$_1$ complex showing the time evolution of the ESDPT reaction through a hydrogen-bonded network within 78 fs. Normal (N), proton transfer (PT), and tautomer (T).

source not of PT processes, but HT processes. However, back-PT reaction was also observed in some trajectories. Thus, the reaction probability of PT is 54%. The details of the PT process can be illustrated by means of a selected trajectory (Figure 3). The numbering atom is the same as defined in Figure 1a. A normal (N) form is observed at 0 fs. The H1 atom departs from the pyrrole ring of 7AI to the O1 atom of methanol (PT1) at 42 fs, then the H2 atom of methanol moves to the N2 acceptor of the 7AI molecule (PT2) at 60 fs until the tautomer (T) form is achieved within 78 fs. After that, 7AI and MeOH fragments separate from each other. Average values for energy and geometric parameters for the 54 trajectories following the ESDPT reaction are shown in Figure 4. The evolution of the average values of two breaking bonds (N1−H1 and O1−H2) and two forming bonds (H1···O1 and H2···N2) is shown in Figure 4a. The intersection between the curves indicates that the first PT occurs at 71 fs when N1−H and H1−O1 bond lengths are equal to 1.361 Å, while the second PT occurs at 84 fs when O1−H2 and H2−N2 are equal to 1.379 Å (listed in Table 2). This time reversal (∼13 fs) between the first and second PT characterizes the process as a concerted double proton transfer. Figure 4b shows that the average energy difference between S_1 and S_0 gradually decreases in the first 100 fs. After that, the average energy difference is still higher than 2 eV, suggesting that the structure of 7AI remains planar throughout the process.[43] This planarity of the 7AI skeleton is confirmed by the average value of the dihedral angle N1C1N2C2, which remains around 180° throughout the simulations as shown in Figure 4c.

It is interesting to compare the 7AI(MeOH)$_1$ cluster with the similar 7AI(H_2O)$_1$ cluster reported by Kina et al.[31] Their results clearly revealed that the proton is transferred from H_2O to 7AI via the N···H hydrogen bond, whereas our results show the opposite way in which the proton is transferred from 7AI to MeOH via N···H hydrogen bond. This difference might be from the hydrogen bonding acid/base abilities of water and methanol. The acidity of a hydrogen bond in water is higher than that of methanol, which

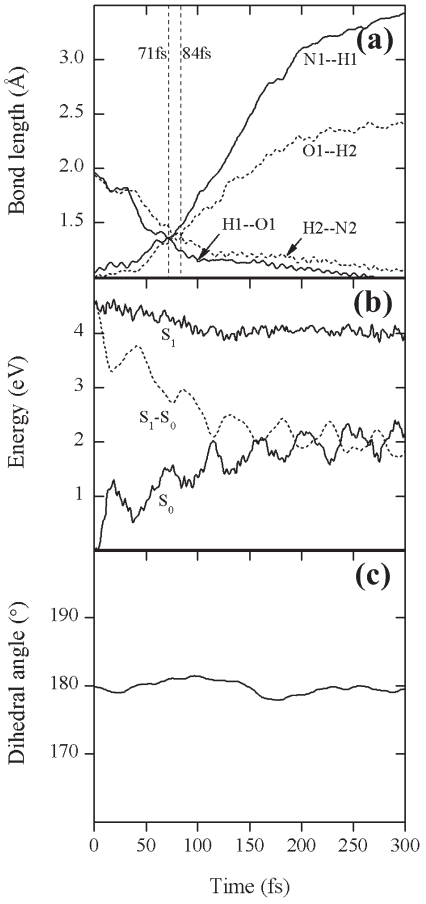

Figure 4. Average values over 54 trajectories of a 7AI(MeOH)$_1$ complex. (a) Average breaking and forming of bonds showing time evolution. (b) Average relative energies of excited state (S_1), ground state (S_0), and energy difference of S_1 and S_0 state ($S_1 - S_0$). (c) Average N1C1N2C2 dihedral angle.

leads to the increased lability of the proton in water than in the methanol. So the first proton in our 7AI(MeOH)$_1$ moves from the 7AI (pyrrole moiety), not the opposite way like in the case of 7AI(H_2O)$_1$. Therefore, the time evolution of PT in 7AI(MeOH)$_1$ is 84 fs, which is 34 fs slower than that in the 7AI(H_2O)$_1$, due to the decreased lability of the proton in methanol compared to that in water.

3.2.2. 7AI(MeOH)$_2$ complex. The ESTPT reaction occurred in 67 out of 100 trajectories, while no reaction was observed in 27 trajectories, and 6 trajectories reached a region of degeneracy of $S_{\pi\pi^*}/S_{\pi\sigma^*}$. Therefore, the probability is 67%, which is higher than that of the 7AI(MeOH)$_1$ complex (see Table 2). A selected trajectory (Figure 5) reveals that the ESTPT reaction takes place within 75 fs. The important numbering atoms assigned in Figure 1b are also adapted to describe this ESTPT reaction. Starting from normal form (N) at 0 fs, the process is summarized in the following three steps: (1) H1 departs from N1 to O1 (PT1) at 42 fs, (2) H2 moves from the O1 to the O2 of methanol (PT2) at 52 fs, and (3) H3 leaves from the O2 of methanol to the N2 of the 7AI molecule (PT3) at 57 fs until the tautomerization (T) with methanol assistance is reached. The complete ESTPT reaction is obtained after 57 fs and followed by the separation of 7AI and MeOH fragments.

dx.doi.org/10.1021/jp2059936 |*J. Phys. Chem. A* 2011, 115, 14129–14136

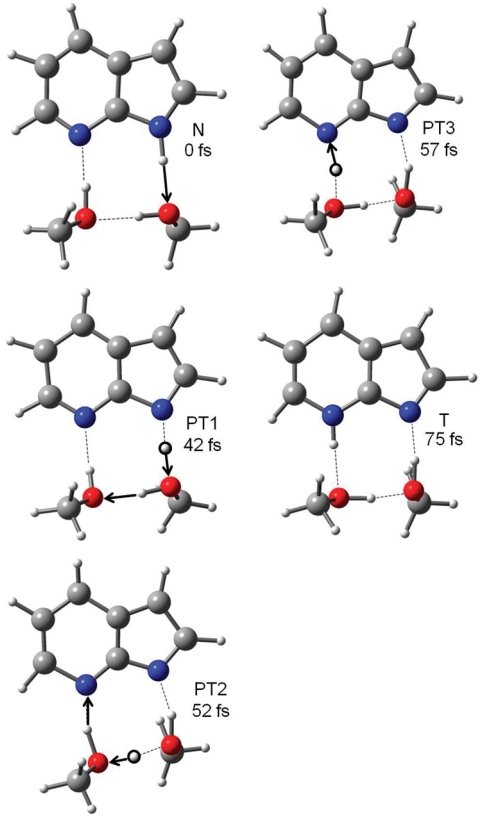

Figure 5. Snapshots for a selected trajectory for a 7AI(MeOH)$_2$ complex showing the time evolution of the ESTPT reaction through a hydrogen-bonded network within 75 fs. Normal (N), proton transfer (PT), and tautomer (T).

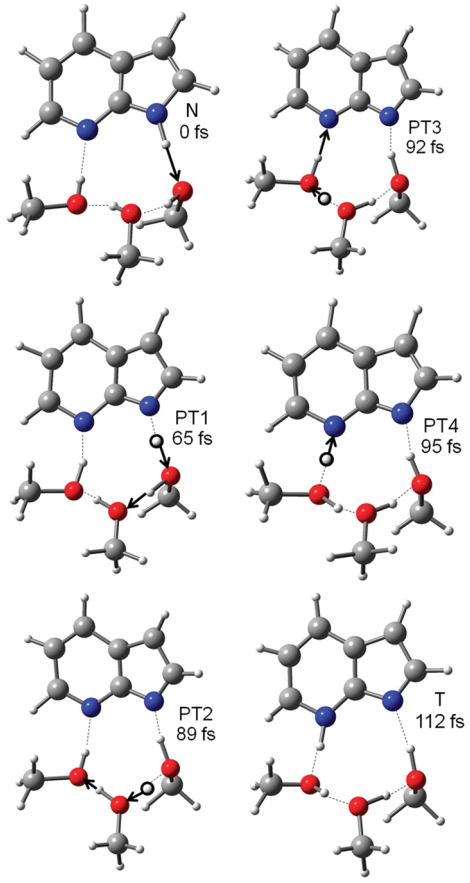

Figure 6. Snapshots for a selected trajectory for a 7AI(MeOH)$_3$ complex showing the time evolution of the ESQPT reaction through a hydrogen-bonded network within 112 fs. Normal (N), proton transfer (PT), and tautomer (T).

The average values over 67 trajectories of the three breaking bonds (N1−H1, O1−H2, and O2−H3) increase rapidly, and, at the same time, the average values of the forming bonds decrease (see Figure S3 in the Supporting Information and Table 2). The first PT process occurs at 57 fs when the average N1−H and H1−O1 distances are equal to 1.297 Å. The distance between the N1 and O1 atoms of 7AI(MeOH)$_2$ cluster while the proton is transferred is shorter than that of the 7AI(MeOH)$_1$ by 0.064 Å. This shorter distance facilitates the movement of the proton from the NH on the five-membered ring on 7AI to OH on methanol in the 7AI(MeOH)$_2$ cluster. The second proton transfers to another methanol at 70 fs when the average O1−H2 and H2−O2 distances are equal to 1.295 Å. The last PT occurs at 83 fs when the average O2−H3 and H3−N2 distances are equal to 1.341 Å (collected in Table 2). There is a certain time lag (∼13 fs) between the first PT and second PT, and the exact same time lag (∼13 fs) between the second PT and third PT. This dynamics behavior indicates a concerted asynchronous process. It is also worth comparing our dynamics simulation results with those of the 7AI(H$_2$O)$_2$ system by Kina et al.[31] Their result shows that the triple-H(proton)-transfer occurs in the time range of 40 to 60 fs but our results with 7AI(MeOH)$_2$ system is in the time range of 57 to 83 fs. Our results support the prediction that by substituting water by methanol into 7AI, the complete PT process would be slower due to the lower polarity of methanol compared to water. In addition, the relative energy difference of S_1-S_0 gradually decreases as the simulation proceeds. After the complete PT process, the average relative energy difference is still higher than 2 eV, suggesting that the structure is planar throughout the PT process. In addition, the average dihedral angle (N1C1N2C2) of 7AI is also 180°, confirming that its skeleton structure is almost planar.

3.2.3. 7AI(MeOH)$_3$ Complex. For 7AI(MeOH)$_3$, there are four hydrogen bonds in the cyclic network. We found that 26 trajectories exhibit the excited-state quadruple proton transfer (ESQPT) reaction, while 60 trajectories exhibit no reaction within the simulation time. Fourteen trajectories proceeded through $S_{\pi\pi^*}/S_{\pi\sigma^*}$ crossing. Thus, the PT reaction probability of this complex is 26% (Table 2). The important numbering atoms as assigned in Figure 1c are also adapted to describe this ESQPT reaction. A selected trajectory of the 7AI(MeOH)$_3$ cluster (Figure 6) exhibits the ESQPT reaction as the proton moves along the hydrogen-bonded network. The normal form (N) exists at 0 fs, and the first (PT1), second (PT2), third (PT3), and fourth (PT4) PT processes occur at 65, 89, 92, and 95 fs, respectively, until the tautomer (T) is formed. As the same criteria was used in 7AI(MeOH)$_{n=1,2}$ complexes, we found that for 7AI(MeOH)$_3$ the average times are 66 (N1−H1 = H1−O1), 77 (O1−H2 = H2−O2), 83 (O2−H3 = H3−O3), and 84 fs (O3−H4 = H4−N2) with bond distances of 1.301, 1.299, 1.270, and 1.338 Å, respectively (see Figure S4 in the Supporting Information and Table 2). All time lags between each PT are less than 10 fs, implying that a concerted mechanism is also favorable for this cluster. The average relative energy difference is

also higher than 2 eV, and the average dihedral angle is 180°, showing that the planarity of 7AI is maintained with no twist in its structure throughout the simulation time.

The average bond breaking and forming intersection can be used to represent PT time evolution in which the type of proton transfer can be distinguished to be either concerted or stepwise mechanisms depending on the PT time interval. If time differences of each PT are less than the fluctuation period time of about 10−15 fs corresponding to normal vibration of N−H and O−H hydrogen bond stretching modes, the concerted mechanism (the proton moves continuously and very rapidly) is involved. The time interval of each PT for 7AI(MeOH)$_n$ (n = 1−3) complexes is less than 15 fs implying that the concerted mechanisms are preferable. Although different types of the ESPT mechanisms and also reaction probability are cluster-size dependent, the phototautomerization of all complexes is achieved with a short time of 84 fs.

4. CONCLUSIONS

We have computed the ground-state structures of 7AI(MeOH)$_n$ (n = 1−3) clusters at the RI-ADC(2)/SVP-SV(P) level. It was found that intermolecular hydrogen bonds between 7AI and methanol molecules increase or become stronger when the number of methanol molecules increases. The excited-state investigations of these complexes have revealed that the ESPT reactions are ultrafast reactions, taking place within less than 100 fs. The ESPT takes place along the PT pathways, confirmed by no crossing between $S_{\pi\pi^*}$ and $S_{\pi\sigma^*}$ states, independently of the cluster size. The time lag between each PT in 7AI(MeOH)$_{n=1-3}$ complexes becomes shorter with increasing number of methanol molecules due to shorter distances between heavy atoms in the cyclic network. In this case, the proton can migrate easily from the proton donor to the acceptor. The ESmultiPT process is cluster-size dependent even though the PT cycle of all complexes is finished within 84 fs. In particular, two methanol molecules can assist and promote the ESTPT reaction most efficiently among the other complexes. In addition, this study has revealed that methanol assistance plays an important role in excited-state PT dynamics. Finally, the RI-ADC(2) method with a relatively modest basis set proved to be an efficient method to investigate PT dynamics in these molecules.

■ ASSOCIATED CONTENT

Supporting Information. Cartesian coordinates of ground-state optimized structures for 7AI(MeOH)$_{n=1-3}$ complexes at RI-ADC(2)/SVP-SV(P) level. Potential energy diagrams of selected trajectories for 7AI(MeOH)$_{1,3}$ complexes at ground state (S_0) and excited states ($S_{\pi\pi^*}$, $S_{\pi\sigma^*}$). (a) Average breaking and forming bonds showing time evolution; (b) average relative energies of excited state (S_1), ground state (S_0), and energy difference of S_1 and S_0 state (S_1-S_0); (c) average dihedral angle of N1C1N2C2 of 7AI(MeOH)$_{2,3}$ complexes. This material is available free of charge via the Internet at http://pubs.acs.org.

■ AUTHOR INFORMATION

Corresponding Author

*E-mail: naweekung@hotmail.com. Phone: +66-53-943341, ext 101. Fax: +66-53-892277.

■ ACKNOWLEDGMENT

The authors wish to thank the National Research University Project under Thailand's Office of the Higher Education Commission for financial support. R.D. gratefully acknowledges the Research Professional Development Project under the Science Achievement Scholarship of Thailand (SAST), Faculty of Science, Chiang Mai University. The Graduate School of Chiang Mai University is also acknowledged. Support was also provided by the Robert A. Welch Foundation under Grant No. D-0005.

■ REFERENCES

(1) Arnaut, L. G.; Formosinho, S. J. *J. Photochem. Photobiol., A* **1993**, *75*, 1.
(2) Formosinho, S. J.; Arnaut, L. G. *J. Photochem. Photobiol., A* **1993**, *75*, 21.
(3) Cohen, B. E.; Pralle, A.; Yao, X.; Swaminath, G.; Gandhi, C. S.; Jan, Y. N.; Kobilka, B. K.; Isacoff, E. Y.; Jan, L. Y. *Proc. Nat. Acad. Sci. U.S. A.* **2005**, *102*, 965.
(4) Kim, T.-I.; Kang, H. J.; Han, G.; Chung, S. J.; Kim, Y. *Chem. Commun. (Cambridge, U. K.)* **2009**, 5895.
(5) Morales, A. R.; Schafer-Hales, K. J.; Yanez, C. O.; Bondar, M. V.; Przhonska, O. V.; Marcus, A. I.; Belfield, K. D. *ChemPhysChem* **2009**, *10*, 2073.
(6) Rodembusch, F. S.; Leusin, F. P.; da Costa Medina, L. F.; Brandelli, A.; Stefani, V. *Photochem. Photobiol. Sci.* **2005**, *4*, 254.
(7) Zimmer, M. *Chem. Rev. (Washington, DC, U. S.)* **2002**, *102*, 759.
(8) Zhang, C.-R.; Liu, Z.-J.; Chen, Y.-H.; Chen, H.-S.; Wu, Y.-Z.; Yuan, L.-H. *J. Mol. Struct. (THEOCHEM)* **2009**, *899*, 86.
(9) M'Baye, G.; Klymchenko, A. S.; Yushchenko, D. A.; Shvadchak, V. V.; Ozturk, T.; Mély, Y.; Duportail, G. *Photochem. Photobiol. Sci.* **2007**, *6*, 71.
(10) Chou, P. T.; Studer, S. L.; Martinez, M. L. *Appl. Spectrosc.* **1991**, *45*, 513.
(11) Chang, S. M.; Tzeng, Y. J.; Wu, S. Y.; Li, K. Y.; Hsueh, K. L. *Thin Solid Films* **2005**, *477*, 38.
(12) Chang, S. M.; Hsueh, K. L.; Huang, B. K.; Wu, J. H.; Liao, C. C.; Lin, K. C. *Surf. Coat. Technol.* **2006**, *200*, 3278.
(13) Gordon, M. S. *J. Phys. Chem.* **1996**, *100*, 3974.
(14) Kyrychenko, A.; Stepanenko, Y.; Waluk, J. *J. Phys. Chem. A* **2000**, *104*, 9542.
(15) Kyrychenko, A.; Waluk, J. *J. Phys. Chem. A* **2006**, *110*, 11958.
(16) Mente, S.; Maroncelli, M. *J. Phys. Chem. A* **1998**, *102*, 3860.
(17) Waluk, J. *Acc. Chem. Res.* **2003**, *36*, 832.
(18) Nosenko, Y.; Kunitski, M.; Thummel, R. P.; Kyrychenko, A.; Herbich, J.; Waluk, J.; Riehn, C.; Brutschy, B. *J. Am. Chem. Soc.* **2006**, *128*, 10000.
(19) Nosenko, Y.; Kyrychenko, A.; Thummel, R. P.; Waluk, J.; Brutschy, B.; Herbich, J. *Phys. Chem. Chem. Phys.* **2007**, *9*, 3276.
(20) Nosenko, Y.; Kunitski, M.; Riehn, C.; Thummel, R. P.; Kyrychenko, A.; Herbich, J.; Waluk, J.; Brutschy, B. *J. Phys. Chem. A* **2008**, *112*, 1150.
(21) Fernández-Ramos, A.; Martínez-Núñez, E.; Vázquez, S. A.; Ríos, M. A.; Estévez, C. M.; Merchán, M.; Serrano-Andrés, L. *J. Phys. Chem. A* **2007**, *111*, 5907.
(22) Guglielmi, M.; Tavernelli, I.; Rothlisberger, U. *Phys. Chem. Chem. Phys.* **2009**, *11*, 4549.
(23) Park, S.-Y.; Jang, D.-J. *J. Am. Chem. Soc.* **2009**, *132*, 297.
(24) Moog, R. S.; Maroncelli, M. *J. Phys. Chem.* **1991**, *95*, 10359.
(25) Gai, F.; Rich, R. L.; Chen, Y.; Petrich, J. W. *ACS Symp. Ser.* **1994**, *568*, 182.
(26) Ilich, P. *J. Mol. Struct.* **1995**, *354*, 37.
(27) Hara, A.; Sakota, K.; Nakagaki, M.; Sekiya, H. *Chem. Phys. Lett.* **2005**, *407*, 30.
(28) Kwon, O.-H.; Jang, D.-J. *J. Phys. Chem. B* **2005**, *109*, 20479.
(29) Sakota, K.; Inoue, N.; Komoto, Y.; Sekiya, H. *J. Phys. Chem. A* **2007**, *111*, 4596.

(30) Sakota, K.; Komoto, Y.; Nakagaki, M.; Ishikawa, W.; Sekiya, H. *Chem. Phys. Lett.* **2007**, *435*, 1.
(31) Kina, D.; Nakayama, A.; Noro, T.; Taketsugu, T.; Gordon, M. S. *J. Phys. Chem. A* **2008**, *112*, 9675.
(32) Taylor, C. A.; El-Bayoumi, M. A.; Kasha, M. *Proc. Natl. Acad. Sci. U.S.A.* **1969**, *63*, 253.
(33) Koizumi, Y.; Jouvet, C.; Norihiro, T.; Ishiuchi, S.-i.; Dedonder-Lardeux, C.; Fujii, M. *J. Chem. Phys.* **2008**, *129*, 104311/1.
(34) Casadesús, R.; Moreno, M.; Lluch, J. M. *Chem. Phys.* **2003**, *290*, 319.
(35) Duong, M. P. T; Kim, Y. *J. Phys. Chem. A* **2010**, *114*, 3403.
(36) Folmer, D. E.; Wisniewski, E. S.; Stairs, J. R.; Castleman, A. W. *J. Phys. Chem. A* **2000**, *104*, 10545.
(37) Sakota, K.; Jouvet, C.; Dedonder, C.; Fujii, M.; Sekiya, H. *J. Phys. Chem. A* **2010**, *114*, 11161.
(38) Sakota, K.; Komure, N.; Ishikawa, W.; Sekiya, H. *J. Chem. Phys.* **2009**, *130*, 224307/1.
(39) Sakota, K.; Kageura, Y.; Sekiya, H. *J. Chem. Phys.* **2008**, *129*, 054303/1.
(40) Kageura, Y.; Sakota, K.; Sekiya, H. *J. Phys. Chem. A* **2009**, *113*, 6880.
(41) Chen, H.-Y.; Young, P.-Y.; Hsu Sodio, C. N. *J. Chem. Phys.* **2009**, *130*, 165101.
(42) Aquino, A. J. A.; Lischka, H.; Hättig, C. *J. Phys. Chem. A* **2005**, *109*, 3201.
(43) Barbatti, M.; Aquino, A. J. A.; Lischka, H.; Schriever, C.; Lochbrunner, S.; Riedle, E. *Phys. Chem. Chem. Phys.* **2009**, *11*, 1406.
(44) Plasser, F.; Barbatti, M.; Aquino, A. J. A.; Lischka, H. *J. Phys. Chem. A* **2009**, *113*, 8490.
(45) Aquino, A. J. A.; Plasser, F.; Barbatti, M.; Lischka, H. *Croat. Chem. Acta* **2009**, *82*, 105–114.
(46) Schriever, C.; Barbatti, M.; Stock, K.; Aquino, A. J. A.; Tunega, D.; Lochbrunner, S.; Riedle, E.; de Vivie-Riedle, R.; Lischka, H. *Chem. Phys.* **2008**, *347*, 446.
(47) Tanner, C.; Manca, C.; Leutwyler, S. *Science (Washington, DC, U. S.)* **2003**, *302*, 1736.
(48) Tanner, C.; Manca, C.; Leutwyler, S. *J. Chem. Phys.* **2005**, *122*, 204326/1.
(49) Ashfold, M. N. R.; Cronin, B.; Devine, A. L.; Dixon, R. N.; Nix, M. G. D. *Science (Washington, DC, U. S.)* **2006**, *312*, 1637.
(50) Kungwan, N.; Plasser, F.; Aquino, A. J. A.; Barbatti, M.; Wolschann, P.; Lischka, H. To be submitted for publication.
(51) Barbatti, M.; Granucci, G.; Persico, M.; Ruckenbauer, M.; Vazdar, M.; Eckert-Maksic, M.; Lischka, H. *J. Photochem. Photobiol., A* **2007**, *190*, 228.
(52) Antol, I.; Vazdar, M.; Barbatti, M.; Eckert-Maksic, M. *Chem. Phys.* **2008**, *349*, 308.
(53) Ahlrichs, R.; Bär, M.; Häser, M.; Horn, H.; Kölmel, C. *Chem. Phys. Lett.* **1989**, *162*, 165.
(54) Ahlrichs, R.; Bär, M.; Häser, M.; Kölmel, C.; Sauer, J. *Chem. Phys. Lett.* **1989**, *164*, 199.
(55) Hättig, C. *J. Chem. Phys.* **2003**, *118*, 7751.
(56) Hättig, C. *Adv. Quantum Chem.* **2005**, *50*, 37.
(57) Schäfer, A.; Horn, H.; Ahlrichs, R. *J. Chem. Phys.* **1992**, *97*, 2571.
(58) Barbatti, M.; Aquino, A. J. A.; Lischka, H. *Phys. Chem. Chem. Phys.* **2010**, *12*, 4959.
(59) Barbatti, M.; Granucci, G.; Ruckenbauer, M.; Pittner, J.; Persico, M.; Lischka, H. *NEWTON-X: A package for Newtonian dynamics close to the crossing seam*, version 1.1, 2007 (www.newtonx.org).